Draft version December 6, 2022
Typeset using LaTeX default style in AASTeX631

A Feasibility Analysis of Constraining Orbital Precession Driven by Mutual Inclination Through Long-Cadence Kepler Light Curves

ABSTRACT

The feasibility of constraining orbital precession of Kepler planets through mutual inclination and impact parameters is analysis. This research targets the exoplanets that obtained a secular changes of impact parameters due to its mutual inclination with other planets in the system. We have derived the relationship between theoretical signal to noise ratio of such planets with its planet-star ratio and impact parameters. The changing of impact parameters with adjacent planets of different period and masses are computed to demonstrate is significance. We have further speculated the population of those planets among all Kepler planets based on two different model. We finally search for varies of Kepler planets and applied the linear function of the impact parameters and Bayes inference maxima likelihood function to get accurate parameters for multiple Kepler planets and analysis the corresponding accuracy statistically. We present following candidates(koi 44.01,koi 192.01, koi 3614.01, koi 6730.01, koi 6663.01, and koi 6677.01) that demonstrate strong Signal to Noise ratio, clean light curve, and significant z-score for the existence long term linear changes of impact parameters. By constraining orbital precession, we can not only optimize the parameters of confirmed Kepler planets, but also speculate the existence of non − transit planets in the Kepler system.

Keywords: Exoplanets Detection — Mutual Inclination — Transit Duration Variation — Impact Parameters

1. INTRODUCTION

Since the start of civilization, human never extinguish the curiosity to the outer space. With the launching of Kepler telescope, enormous breakthrough took place in the understanding of exoplanets by identifying thousands of more confirmed planets, optimizing the parameters Batalha et al. (2013), and reveals the general statistic of exoplanets along with their system Fang & Margot (2012).

Majority of the exoplanets are detected by observed the changes of flux of the star in the system Borucki et al. (2010). All of the planets in the system will transit from the star in our telescopes requires those planets approximate co-planar (relatively low mutual inclination angle). Even though majority of the Kepler system follows this pattern, a portion of system still obtained larger inclination angle Zhu & Dong (2021), which will cause the transit of some exoplanets in the system not visible by earth telescope. Due to the existence of non - transiting planets, there is a significant distinction between detected and expected number of Kepler planets, which is known as the Kepler dichotomy. To resolve this, we have attempted to detect the non-transit planets by observing their gravitational influence on transit planets via the constrains of mutual inclination.

Mutual Inclination is more significance in planets with short period that placed in a close pack system that composed of other large mass planets, which are commonly exists in the Kepler population as revealed by Batalha et al. (2013), Borucki et al. (2011), Borucki et al. (2010), and Fabrycky et al. (2014). Because of their large distribution, varies previous research has combined mutual inclination with Transit Time Variation Hadden & Lithwick (2014) Judkovsky et al. (2020), Transit Duration Variation from orbital precession Hamann et al. (2019), and Radial Velocity survey Tremaine & Dong (2012), to discover the non-transit planet.

Nevertheless, Transit Duration Variation result from the secular changes of impact parameter are usually ignored in the previous research beside a very recent publication Millholland et al. (2021), who applied the distribution of the impact parameter changes to constrain the mutual inclination distribution of Kepler planets. Impact parameters can change because of various effects: the uneven distribution of gravity due to the inclination angle and eccentricity, the changing of the period due to orbital resonance, and the variation of the semi-major axis that resulted from transit time variation. Therefore, the study of impact parameters combined with transit time variation can help us understand further improve planetary parameters. Regardless both Millholland et al. (2021) and us study the feasibility of transit duration variation, Millholland et al. (2021) approximated the distribution of target planets via n-body integration with Angular Momentum Deficit and Two Rayleigh Model, while this paper approach from two different models, and provides with more potential planet candidates that demonstrates long term changes of impact parameters.

Within the paper, section II presented our calculation of theoretical Signal to Noise Ratio of planets with secular changing of impact parameters, section III reveals the derivation of impact parameters changes from their mutual inclination and the perturbation of two planet system and estimated the relative frequency of those planets in the Kepler population from two different model, section IV demonstrates our process in light kurve modeling, and section V present our discussion and conclusion.

2. THEORETICAL SIGNAL TO NOISE RATIO

While a planet is transiting in front of the star, a portion of the light from the star will be blocked by the planet. The changing of the flux from the star can be approximated from the size and the position of the planets relative to the star based on the equations from Mandel & Agol (2002) that presented below.

$$F = 1 - \frac{1}{\pi}(p^2\kappa_0 + p^2\kappa_1 - \sqrt{\frac{4z^2 - (z + z^2 - p^2)^2}{4}}) \tag{1}$$

with

$$\begin{cases} \kappa_1 = \cos^{-1}(\frac{1-p^2+z^2}{2z}) \\ \kappa_0 = \cos^{-1}(\frac{p^2+z^2-1}{2pz}) \end{cases} \tag{2}$$

Because the equation is designed to analysis the flux from the star during the planet is transiting, it valid when $\mid 1-p \mid < z < 1+p$. By defining r_p as the radius of the planet and r_* as the stellar radius, we can derive the size ratio p and normalized separation of the centers z follow:

$$\begin{cases} p = \frac{r_p}{r_*} \\ z = \frac{d}{r_*} \end{cases} \tag{3}$$

d stands for center-to-center distance between the star and the planet which can be expanded into vertical components b and horizontal components x follow the Pythagorean theorem, $d = \sqrt{b^2 + x^2}$. The vertical components b is known as the impact parameters of the transit parameters, and we define $\dot{b}$ as the changing of impact parameter of the transit planet respect to time.

By assuming the impact parameter only changes linearly respect to time, the flux from the star with $\dot{b}$ as a finite non-zero number, $F_b\,(x, b)$, can be approximated from the flux of the star that obtained the planet with no changing of impact parameter through time, $F\,(x, b)$:

$$F_b(x, b) \approx f(x, b) + \frac{\partial F(x, b)}{\partial b}\Delta b \tag{4}$$

Δb means the changing of impact parameters in the given time that can be derived from, N_T, the number of orbits that the planets have completed, and T, the period of the planets:

$$\Delta b = \dot{b} N_T T \tag{5}$$

N_T is the number of transits in the given period which equals to the reciprocal of the period. The mean difference of $F_b\,(x, b)$ and $F\,(x, b)$, $\langle \delta F^2 \rangle$ can be computed from

Table 1. Notation Table

Notation	Description
(1)	(2)
t	time
a	semi-major axis
b	Impact Parameters
R_*	radius of the star
M_*	mass of the star
m	mass of the planet
W	window for savigol
δ_t	time interval of short-cadence of Kepler Telescope
t_0	Transit Epoch
$\dot{b}$	The changing of impact parameters respect to time
T	Period
p	Planet-star ratio
u_1	Limb Darkening Parameter 1
u_2	Limb Darkening Parameter 2
ρ_*	$\frac{M_*}{r_*^3}$, the density of the star
ω	orbital frequency
$\overrightarrow{\Theta}$	Parameter Vector for Light curve deternding
$\overrightarrow{\Theta}_b$	$\overrightarrow{\Theta}$ when b is changing
$\overrightarrow{\Theta}^{(n)}$	$\overrightarrow{\Theta}$ after nth optimization
n	number of data points
N	number of planets in that system
N_T	number of transits
z	normalized separation between centers
$\bar{F}$	raw flux from kepler telescope
$\hat{F}$	Model flux generated from $\overrightarrow{\Theta}$
F	Actual flux from Kepler telescope
σ	Standard deviation for the error of the F and $\hat{F}$
σ_b	Standard deviation for the error of $\hat{F}(\overrightarrow{\Theta}_b)$ and$\hat{F}(\overrightarrow{\Theta})$
σ_I	Standard deviation for the inclination of planets

$$\langle \delta F^2 \rangle \approx \frac{1}{x_{max} - x_{min}} \int_{x_{min}}^{x_{max}} (\frac{\partial F(x,b)}{\partial b} \Delta b)^2 \mathrm{d}x \tag{6}$$

$$= \frac{1}{2(1+p)} \int_{-1-p}^{1+p} (\frac{\partial F(x,b)}{\partial b} \frac{\mathrm{d}b}{\mathrm{d}t} T N_T)^2 \mathrm{d}x \tag{7}$$

Theoretical signal to noise ratio is given by the sum of the difference of all data points in the two models relative to their variance:

$$\mathrm{SNR}^2 = \sum_{i=0}^{n} \frac{(F_b(z_i) - F(z_i))^2}{\sigma_b^2} \tag{8}$$

$$= \langle \delta F^2 \rangle (\frac{\tau}{\delta_t}) \frac{1}{2\sigma_b^2} \tag{9}$$

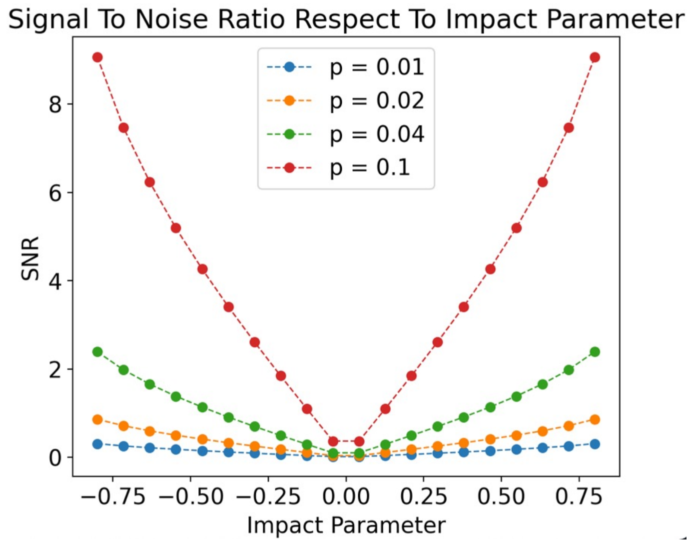

Figure 1. In the figure above, the calculation follows the flux equation given by Mandel & Agol (2002) and assume the changes of impact parameters can be approximated via linear model. y-axis is the impact parameter and x-axis are the Signal Noise Ratio. The colorful lines represent results of different planet-star ratios respectively.

δ_t is the short cadence of the Kepler telescope that equals to 2 minutes, and σ_b is assumed to be 8e-4. Finally, the graph of Signal to Noise Ratio respect to the impact parameters of planets with four different planet – star ratio was plotted in figure 1.

3. PERTURBATIONS OF TWO PLANET SYSTEM

In this section, we simulate the perturbations of varies artificial two body systems. Section 3.1 derived the changing of impact parameters from the mutual inclination with its adjacent planets. Section two simulated the two planets system that based on the calculation of 3.1

3.1. *Derivation From Mutual Inclination*

We derives the therotical changing of impact parameters of Kepler planets from their periodical changes of The changing of the impact parameter of the transit planet, $\dot{b}$, can be calculated from the changing of its mutual inclination with another planet in the system, $\frac{\mathrm{d}I}{\mathrm{d}t}$, and its semi-major axis, a:

$$\dot{b} = \frac{a}{r_*} \mid \frac{\mathrm{d}I}{\mathrm{d}t} \mid \tag{10}$$

I is the complex inclination that defined from the inclination, θ,and longitude of ascending node, Ω:

$$I = \theta e^{i\Omega} \tag{11}$$

For planets j and planets k, assuming planet j is close to the star, their rate of inclination change is given by

$$\frac{\mathrm{d}I}{\mathrm{d}t}_{jk} = \omega_{ij} \left(I_j - I_k\right) \tag{12}$$

with ω_{ij} calculated from

$$\omega_{jk} = \frac{G m_j m_k a_j}{a_k^2 L_j} b_{3/2}^{(1)} \left(\alpha\right) \tag{13}$$

in which L_j and $b_{3/2}^{(n)} \left(\alpha\right)$ is derived from

$$L_j = m_j \sqrt{G M_* a_j} \tag{14}$$

and

$$b_{3/2}^{(n)} \left(\alpha\right) = \frac{1}{2\pi} \int_0^{\pi} \frac{\cos\left(nt\right)}{\left(\alpha^2 + 1 - 2\alpha \cos t\right)^{3/2}} \mathrm{d}t \tag{15}$$

which m_i, m_j , and a_i, a_j are the mass and semi-major axis of the two planets respectively, M_* means the mass of the star, and $b_{3/2}^{(n)}(\alpha)$ means Laplace coefficients.

3.2. *Statistical Properties of Kepler Planets*

In the artificial system, the radius of the planets is randomly chosen from all detected Kepler planets, and approximate their mass from the radius following the model of Zhu et al. (2018) by assuming their density close to the earth density:

$$a = \sqrt[3]{T^2 \left(M_* + m\right)} \tag{16}$$

Similarly, the period of the first planets is randomly selected from all Kepler planets. The period for rest of the planets is chosen from the log uniform distribution, with lower limit of 1.3 and upper limit of 4.0, times the period of the first planets. The semi-major axis of each planet is derived from its period, T, and mass, m, follow the Kepler 3rd law:

$$m \approx 3 \cdot 10^{-6}\ r^{2.06} \tag{17}$$

The inclination angle of each planet is randomly choosing from the two-dimensional normal distribution where both real parts and imaginary parts center at zero, with the standard deviation, σ_I, based on the multiplicity distribution (number of planets in the system), N, given by of Zhu et al. (2018) :

$$\sigma_I = 0.7 \left(\frac{N}{5}\right)^{-4} \tag{18}$$

The changing of the impact parameter, $\dot{b}$, of each planet is calculated from the procedures in Section 3.1, beside rate of inclination change is now given by the summation of all pairs of planets interactions.

$$\frac{\mathrm{d}I_j}{\mathrm{d}t} = \sum_{k \neq j}^{N-1} \omega_{jk} \left(I_j - I_k\right) \tag{19}$$

The radius of star and mass of star are selected from all confirmed Kepler Star. Sufficient system with multiplicity distribution that ranged from 2 to 6 has been generated.

Additionally, Lissauer et al. (2011) reveals the multiplicity distribution of Kepler planets can be approximated with Poisson distribution and Fabrycky et al. (2014) suggests at least one half of the Kepler planets obtained mutual inclination that agree with Rayleigh distribution with sigma around 1 to 2 degrees. We introduce another simulation with the inclination angle of each planet is randomly choosing from Rayleigh distribution with σ equals to 2 degrees, and the multiplicity distribution is chosen from Poisson Distribution with mean equals to 3.

The histogram of $\dot{b}$ with relative frequency of each multiplicity distribution is plotted in . We have also recorded the percentage of significant $\dot{b}$, which defined as greater or equal to 0.01. Their relative frequency in the population is presented in 2.

4. LIGHTKURVE MODELING

4.1. *Methodology*

We download the light curve of Kepler planets from kplr library that developed by Foreman-Mackey (2018) along with its existing parameters. We first extract the light curve via Lightkurve Collaboration et al. (2018).We extract the transit by first blocking the transit from the original trend and apply a third-degree polynomial to fit the trend, and then divide the transit by the trend we just fit, to obtain the flux of star. In the end, by assuming the error follows the gaussian distribution, we smooth the flux through Savitzky–Golay filter in Virtanen et al. (2020) and obtained the original flux function, F_0. We assume the flux from the star can be approximated by quadric limb darkening proposed by Mandel & Agol (2002), thus defined the parameters vector of the planets through:

$$\vec{\Theta} = < t_0, b_0, T, p, u_1, u_2, \rho > \tag{20}$$

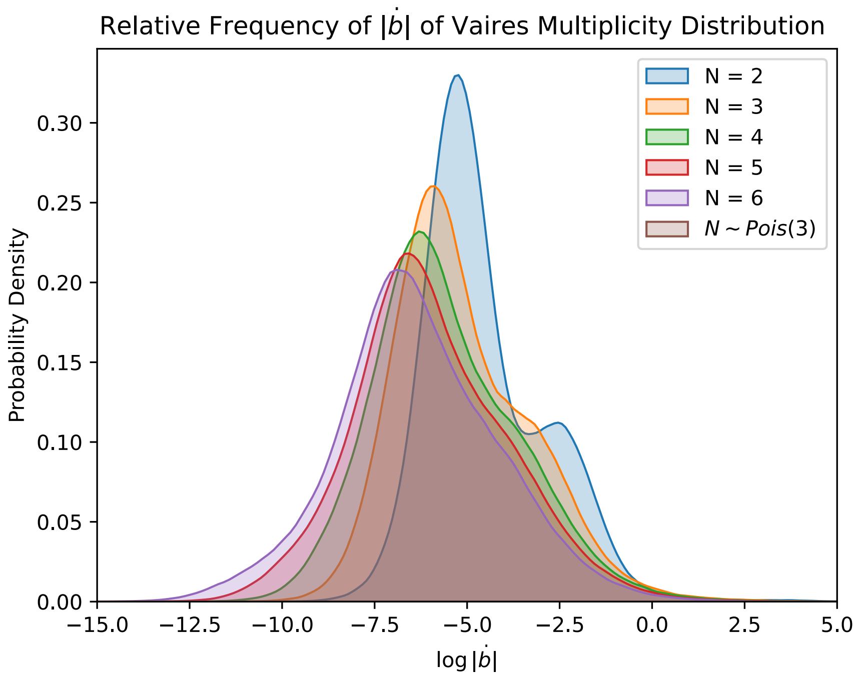

Figure 2. Relative Frequency of | $\dot{b}$ | of Varies Multiplicity Distribution. In the figure above, the x-axis represented magnitude of $\dot{b}$ in the logistic scale, and the y-axis represents their corresponding relative frequency in the population. N means the multiplicity distribution of the system.

Table 1. The Relative Frequency of Significant $\dot{b}$ within Kepler System

model	Multiplicity Distribution	Relative Frequency
(1)	(2)	(3)
Zhu et al. (2018)	$N = 2$	8.598 %
Zhu et al. (2018)	$N = 3$	6.108 %
Zhu et al. (2018)	$N = 4$	4.761 %
Zhu et al. (2018)	$N = 5$	3.806 %
Zhu et al. (2018)	$N = 6$	3.069 %
Lissauer et al. (2011)	$N \sim Pois(3)$	2.016 %

In the notation above, t_0 stands for the transit epoch; b_0 means the initial impact parameters; similar to the previous sections, T and p continues represents the period and planets-star ratio separately, which p is calculated from the square root of transit depth; u1 and u2 are the limb darkening parameters of the star, which are assumed to be 0.25; lastly, ρ is the density of the star, which is assumed to be 1. We first calculated the star radius semi major axis ratio, $\frac{a}{R_*}$, via

$$\frac{a}{R_*} = \sqrt[3]{\frac{GT^2\rho}{3\pi}} \tag{21}$$

We then computed the model flux, $\hat{F}$, from batman libary that developed by Kreidberg (2015).

4.2. *Bayesian Analysis*

According to Bayes inference, the possibility of actual flux, F, given model flux, $\hat{F}$, can be derive from

$$P\left(\mathrm{F}\middle|\hat{\mathrm{F}}\left(\vec{\Theta},\mathrm{t}\right)\right)=\frac{P\left(\hat{\mathrm{F}}\left(\vec{\Theta},\mathrm{t}\right)\middle|\mathrm{F}\right)P\left(\mathrm{F}\right)}{P\left(\hat{\mathrm{F}}\left(\vec{\Theta},\mathrm{t}\right)\right)} \tag{22}$$

Rearrange the equation:

$$P\left(\hat{\mathrm{F}}\left(\vec{\Theta},\mathrm{t}\right)\middle|\mathrm{F}\right)=P\left(\mathrm{F}\middle|\hat{\mathrm{F}}\left(\vec{\Theta},\mathrm{t}\right)\right)\cdot P\left(\hat{\mathrm{F}}\left(\vec{\Theta},\mathrm{t}\right)\right)\cdot\frac{1}{P\left(\mathrm{F}\right)} \tag{23}$$

$P\left(F\right)$is constant due to the observation data are objective and cannot be manipulated; as $P\left(\mathrm{F}\middle|\hat{\mathrm{F}}\left(\vec{\Theta},\mathrm{t}\right)\right)$ is the prior, all underlying models are equally likely to be generated, thus$P\left(\hat{\mathrm{F}}\left(\vec{\Theta},\mathrm{t}\right)\right)$is also constant, which proves $P\left(\hat{\mathrm{F}}\left(\vec{\Theta},\mathrm{t}\right)\middle|\mathrm{F}\right)$ is directly proportional and only depends on $P\left(\hat{\mathrm{F}}\left(\vec{\Theta},\mathrm{t}\right)\middle|\mathrm{F}\right)$. We denote $L=P\left(\mathrm{F}\middle|\hat{\mathrm{F}}\left(\vec{\Theta},\mathrm{t}\right)\right)$. Assume F is only composed with the true signal and random noise that follows the Gaussian distribution, thus the likelihood estimation of $P\left(\mathrm{F}\middle|\hat{\mathrm{F}}\left(\vec{\Theta},\mathrm{t}\right)\right)$can be calculated from:

$$G\left(\vec{\Theta},t\right)=\log L\left(\vec{\Theta},t\right)=-\sum\frac{\left(\hat{F}\left(\vec{\Theta},t\right)-F\right)^2}{2\sigma^2} \tag{24}$$

With

$$\sigma=\sqrt{\frac{\sum\mid F-\hat{F}\left(\vec{\Theta},t\right)\mid}{n}} \tag{25}$$

In which n stands for the number of data points. Thus, minimum the squares of difference between $\hat{F}$ and F will maximum the likelihood estimation of $\hat{F}$.

4.3. *Optimization Via TTV and TDV*

Ideally, the transit of the planets will uniform distributed among its periods. In this situation, the time in the transit, $\widetilde{t}$, can be directly computed from the time of observer, t, follows

$$\widetilde{t}=\left(t-t_0+\frac{T}{2}\right)\mathrm{mod}(T-\frac{T}{2}) \tag{26}$$

However, due to the gravitational influence by the nearby planets in the system. Kepler planets usually experience Transit Time Variation, thus the derivation of $\widetilde{t}$, need to consider the effect of TTV:

$$\widetilde{t}=\left(t-t_0+\frac{T}{2}+TTV\right)\mathrm{mod}(T-\frac{T}{2}) \tag{27}$$

Consequently, we define $G_t\left(\vec{\Theta},t\right)$ that like $G\left(\vec{\Theta},t\right)$ beside the input variable t obtained a new parameter, TTV. We then constructed the model that consider impact parameters experienced secular linear changes respect to time:

$$b\left(t\right)=b_0+\frac{\mathrm{d}b}{\mathrm{d}t}\Delta t \tag{28}$$

Thus, the new parameters vectors, $\vec{\Theta_b}$, will composed one more parameter compare with$\vec{\Theta}$, $\dot{b}$, which stands for $\frac{\mathrm{d}b}{\mathrm{d}t}$:

$$\vec{\Theta_b}=<t_0,b_0,P,R_x,u_1,u_2,\rho,\dot{b}> \tag{29}$$

Similar, the correlate lognormal probability function, $G_b\left(\vec{\Theta_b},t\right)$, is defined as:

$$G_b\left(\vec{\Theta_b},t\right)=-\sum\frac{\left(\hat{F}\left(\vec{\Theta_b},t\right)-F\right)^2}{2{\sigma_b}^2} \tag{30}$$

With

$$\sigma_b = \sqrt{\frac{\sum \mid F - \hat{F}\left(\vec{\Theta_b}, t\right) \mid}{n}} \tag{31}$$

We located the global minimum via basin hopping from Virtanen et al. (2020)] of $G_t\left(\vec{\Theta}, t\right)$, and its corresponding $\vec{\Theta}$ and t, name them $\vec{\Theta}^{(1)}$ and $t^{(1)}$, which the "(1)" in the superscript stands for the 1st iteration. Similarly, we found the global minimum of $G_b\left(\vec{\Theta_b}, t\right)$ and its corresponding $\vec{\Theta}_b^{(1)}$. We then plug those results back to the model function and compare $\hat{F}\left(\vec{\Theta}^{(1)}, t^{(1)}\right)$ and $\hat{F}\left(\vec{\Theta}_b^{(1)}, t^{(1)}\right)$ with the observe flux, F, respectively. Outliers in F are defined as obtained 15 residuals away from the consistent $\hat{F}$ and removed for 2nd iteration.

Lastly, we repeated the process, and obtain $\vec{\Theta}^{(2)}$ and $\vec{\Theta}_b^{(2)}$from the global minimum of $G_t\left(\vec{\Theta}, t\right)$ and $G_b\left(\vec{\Theta_b}, t\right)$.

4.4. *Statistical Power*

The fisher information of $\vec{\Theta_b}$ is calculated by

$$I(\vec{\Theta_b}) = E[-\frac{\mathrm{d}^2}{\mathrm{d}\vec{\Theta_b}^2} G_b\left(\vec{\Theta_b}, t\right)] \tag{32}$$

Therefore, the estimating parameters difference between the two model will form a normal distribution that centers at zero with variance inverse proportional to the fisher information, $\vec{\Theta_b}$, via

$$\sqrt{n}(\vec{\Theta_b} - \vec{\Theta}) \rightarrow N(0, \frac{1}{I(\vec{\Theta_b})}) \tag{33}$$

The corresponding z-score of the difference, $Z_{\Delta G}$ is then computed from the normal distribution presented within equation 30. Similarly, the z-score of $\dot{b}$, $Z_{\dot{b}}$ is derived from equations above. Lastly, we calculate the signal to Noise ratio, , S_r, from equation (15) from Pont et al. (2006)

$$S_r = \alpha^{1/2} p^2 N^{1/2} \delta_t^{1/2} T^{-1/2} \sigma_d^{-1} \tag{34}$$

with p stands for the planet-star radius ratio, N is the number of data points, δ_t is the short cadence time of Kepler telescope, T is the period of the planets, and σ_d is the uncertainty that calculated within equation 33. α is limb darkening parameters which we set into 1.

5. DISCUSSION AND CONCLUSION

Section 5.1 presents our criteria for searching planetary candidates, section 5.2 demonstrates statistical accuracy and light curve of few successful planets, and section 5.3 provide the discussion of our research.

5.1. *Sample Selection For Candidates*

Amongst all Kepler planets, we have three separate criteria on their radius, period, and mass.

1. The mass of the planets must obtain at least four earth mass to ensure the significance of Signal to Noise ratio.
2. The radius of the planets is larger than 0.03 of the star radius to guarantee the the ingress and egress of the light curve will be notable. However, the radius of the planets has to be smaller than 0.1 of the star to ensure the solar flux density will not change inside the planet.
3. The period of the planets is larger than three days to confirm enough data points for each transits, and the period of the planets is smaller than hundred days to secure enough transits to observe the changing of impact parameters.

We therefore implement our algorithms on those candidates, and found few planets obtains strong Signal to Noise ratio, clean light curve, and significant z-score for the existence long term linear changes of impact parameters, present their light curve, and statistical accuracy within the following sections.

Table 2. The Statistical Significance of Satisfied Planets

Planet	Num Transits	Num Data Points	$Z_{\Delta G}$	Z_b	SNR
(1)	(2)	(3)	(4)	(5)	(6)
koi 44.01	8	1365	33.91	12.61	11.44
koi 192.01	30	507	-11.7	7.88	17.94
koi 3614.01	127	1270	14.06	18.63	112.34
koi 6730.01	24	1045	7.08	26.02	122.28
koi 6663.01	18	683	18.82	26.91	60.32
koi 6677.01	39	1313	12.58	24.30	265.78

5.2. *Results*

Koi 44.01 is previously been identified obtains long term linearly changes of impact parameters. We therefore use the short cadence data from koi 44.01 to test our code. After successful, we then utilized our algorithms on the candidates through long cadence data, and found five satisfied planets, which is koi 192.01(figure 5), koi 3614.01 (figure 4), koi 6730.01 (figure 8, and koi 6677.01(figure 7). The statistical result is presented within table 1

All of the satisfied planets have acceptable number of data points and transits, which prove the valid of their parameters and statistical accuracy. We observe both $Z_{\Delta G}$ and Z_b of the satisfied planets are much above two, which proves the changing of impact parameters are very unlikely to happens purely by chance. The high SNR value prove the light curve fitting is success, and therefore noise does not significantly influence their parameters and accuracy.

As we mentioned earlier, Transit Timing variation is limited by planetary inter-eccentricity exchanges and eccentricity-mass degeneracy. Within the above six systems, future researchers can observe their orbital precession from transit duration variation in addition to transit timing variation, and get an independent constraints on mass, eccentricity, and inclination.

5.3. *Discussion*

We discover five planets obtain significance long - term linear changes of impact parameters. Future researchers can utilized this data combine with orbital dynamics to constrain their orbital precession. This can not only optimize their parameters also speculate the potential existence of non – transit planets within their system. Due to the limitation of computational capacities, majority of planets within the research has only been searched with long cadence. Therefore, we propose the applying of short cadence for more accurate parameters and improved statistical significance. There are few limitations regarding of outlier removal process and plotting algorithms, in which we discuss in detail combine with the failure graph within appendix. Within the study, we apply Bayesian inference and log maximal likelihood function find the optimal parameters and removing noise. We recommend the usage of more sophisticated model, eg machine learning and nerve network, for extracting the planetary parameters at further studies. Lastly, we apply linear model to fit the changes of impact parameters, a more complicated and realistic version can be used in future studies.

APPENDIX

Within the appendix, we are going to present some of our failure graph, and discuss their limitations, along with space for improvements.

A. PLOTTING IMPROVEMENT

In order to let us observe the fit result and therefore improving the fitting algorithms, we have plot the outliers on the detrending light curve. However, some of the outliers are not result from our fitting function, but an technical

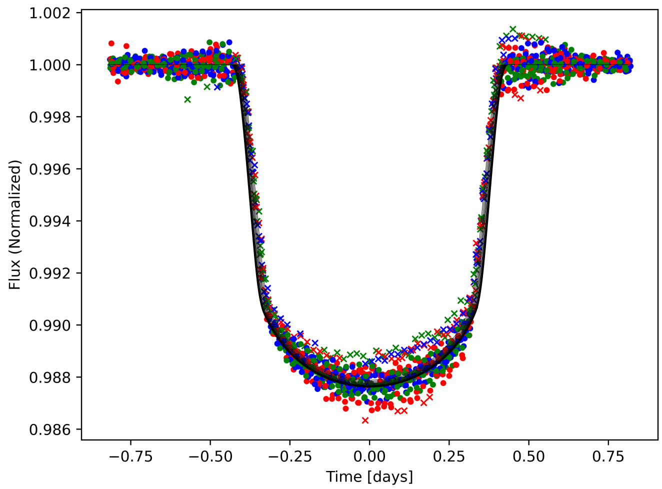

Figure 3. Deterending Light curve for the short-cadence Koi 44.01. The x-axis represents the lasting of each transit in the unit of days, the y-axis represents the normalized flux from the star. Every dot represents a data point from the Kepler telescopes and different colors marked the data points from different transit. The dark lines are the best fit model of each transits.The outliers that are 5 σ away are marked as cross (x).

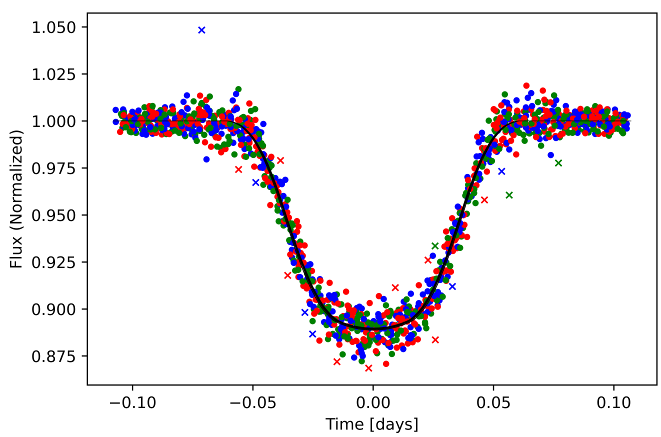

Figure 4. Deterending Lightcurve for the long-cadence Koi 3614.01. The x-axis represents the lasting of each transit in the unit of days, the y-axis represents the normalized flux from the star. Every dot represents a data point from the Kepler telescopes and different colors marked the data points from different transit. The dark lines are the best fit model of each transits.The outliers that are 5 σ away are marked as cross (x).

issue of the Kepler-telescope, eg the screen is dazzled by some outside light source. For example, koi 46.01 at figure 9 demonstrate an acceptable light curve, but due to the graph obtain an unkown flux that obtain 1.04 magnitude of luminosity, the general trend of the light curve has been shrinked, and therefore invisible. Thus, for future plotting, we recommend included the outlier that is within twenty sigma to observe the result of fitting algorithms, but remove all outlier above twenty sigma from the graph.

B. OUTLIER REMOVAL

We found the outlier removal process is overly strict, which sometimes result the whole transit of some planets has been removed as the algorithms define all the data points within the transit as outlier. The z-score of koi 3542.01 at figure 10should be higher than we estimated, as we can observe there few light curves demonstrates significant different depth compare with other light curve, but accidentally not includes within calculation as those data points are crossed and defined as outliers. A more obvious example will be koi 3609.01 at figure 11, in which we observed multiple transits has been removed.

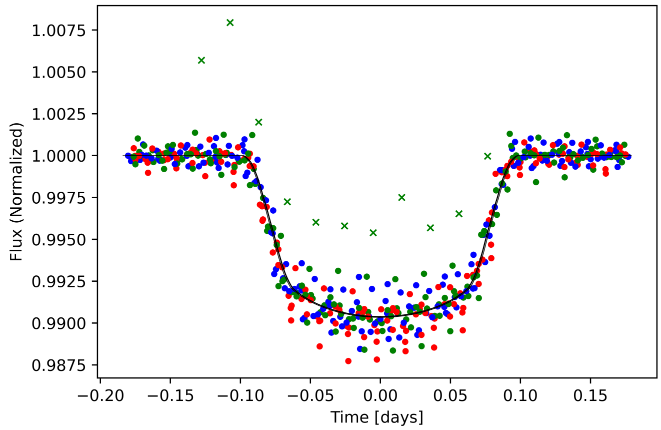

Figure 5. Deterending Lightcurve for the long-cadence Koi 192.01. The x-axis represents the lasting of each transit in the unit of days, the y-axis represents the normalized flux from the star. Every dot represents a data point from the Kepler telescopes and different colors marked the data points from different transit. The dark lines are the best fit model of each transits.The outliers that are 5 σ away are marked as cross (x).

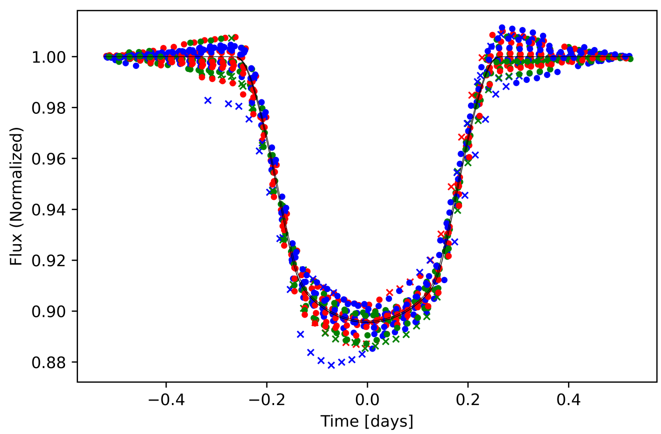

Figure 6. Deterending Lightcurve for the long-cadence Koi 6730.01. The x-axis represents the lasting of each transit in the unit of days, the y-axis represents the normalized flux from the star. Every dot represents a data point from the Kepler telescopes and different colors marked the data points from different transit. The dark lines are the best fit model of each transits.The outliers that are 5 σ away are marked as cross (x).

C. SAMPLE SELECTION IMPROVEMENT

We suggest future candidate selection should be constrained with confirmed planets. Within this research, we notice multiple light curve is not result from a transit planets. For example, koi 6933.01 at figure 12 appears to be star transit a star, as the changing of flux is more than 0.5 of the normalized value.

REFERENCES

Batalha, N. M., Rowe, J. F., Bryson, S. T., et al. 2013, ApJS, 204, 24, doi: 10.1088/0067-0049/204/2/24

Borucki, W. J., Koch, D., Basri, G., et al. 2010, Science, 327, 977, doi: 10.1126/science.1185402

Borucki, W. J., Koch, D. G., Basri, G., et al. 2011, ApJ, 736, 19, doi: 10.1088/0004-637X/736/1/19

Fabrycky, D. C., Lissauer, J. J., Ragozzine, D., et al. 2014, ApJ, 790, 146, doi: 10.1088/0004-637X/790/2/146

Fang, J., & Margot, J.-L. 2012, ApJ, 761, 92, doi: 10.1088/0004-637X/761/2/92

Foreman-Mackey, D. 2018, kplr: Tools for working with Kepler data using Python, Astrophysics Source Code Library, record ascl:1807.027. http://ascl.net/1807.027

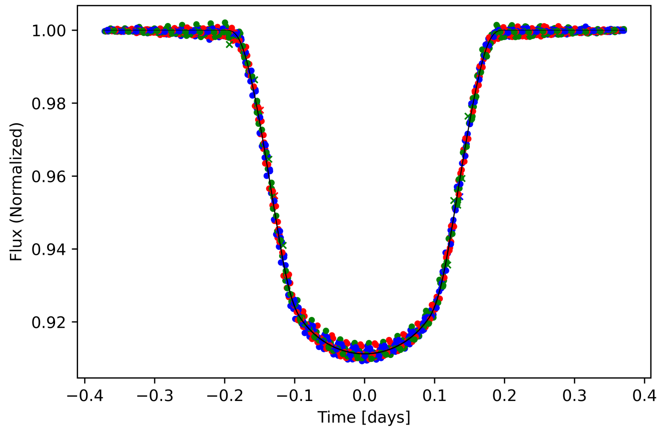

Figure 7. Deterending Lightcurve for the long-cadence Koi 6677.01. The x-axis represents the lasting of each transit in the unit of days, the y-axis represents the normalized flux from the star. Every dot represents a data point from the Kepler telescopes and different colors marked the data points from different transit. The dark lines are the best fit model of each transits.The outliers that are 5 σ away are marked as cross (x).

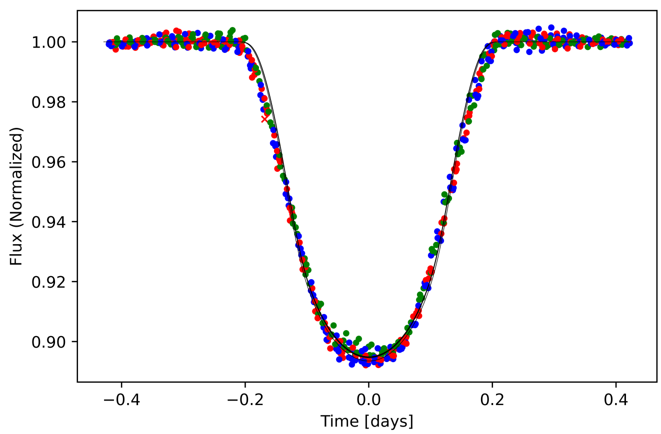

Figure 8. Deterending Lightcurve for the long-cadence Koi 6663.01. The x-axis represents the lasting of each transit in the unit of days, the y-axis represents the normalized flux from the star. Every dot represents a data point from the Kepler telescopes and different colors marked the data points from different transit. The dark lines are the best fit model of each transits.The outliers that are 5 σ away are marked as cross (x).

Hadden, S., & Lithwick, Y. 2014, ApJ, 787, 80, doi: 10.1088/0004-637X/787/1/80

Hamann, A., Montet, B. T., Fabrycky, D. C., Agol, E., & Kruse, E. 2019, AJ, 158, 133, doi: 10.3847/1538-3881/ab32e3

Judkovsky, Y., Ofir, A., & Aharonson, O. 2020, AJ, 160, 195, doi: 10.3847/1538-3881/abb406

Kreidberg, L. 2015, Publications of the Astronomical Society of the Pacific, 127, 1161, doi: 10.1086/683602

Lightkurve Collaboration, Cardoso, J. V. d. M., Hedges, C., et al. 2018, Lightkurve: Kepler and TESS time series analysis in Python, Astrophysics Source Code Library. http://ascl.net/1812.013

Lissauer, J. J., Ragozzine, D., Fabrycky, D. C., et al. 2011, ApJS, 197, 8, doi: 10.1088/0067-0049/197/1/8

Mandel, K., & Agol, E. 2002, ApJL, 580, L171, doi: 10.1086/345520

Millholland, S. C., He, M. Y., Ford, E. B., et al. 2021, AJ, 162, 166, doi: 10.3847/1538-3881/ac0f7a

Pont, F., Zucker, S., & Queloz, D. 2006, Monthly Notices of the Royal Astronomical Society, 373, 231, doi: 10.1111/j.1365-2966.2006.11012.x

Tremaine, S., & Dong, S. 2012, AJ, 143, 94, doi: 10.1088/0004-6256/143/4/94

Virtanen, P., Gommers, R., Oliphant, T. E., et al. 2020, Nature Methods, 17, 261, doi: 10.1038/s41592-019-0686-2

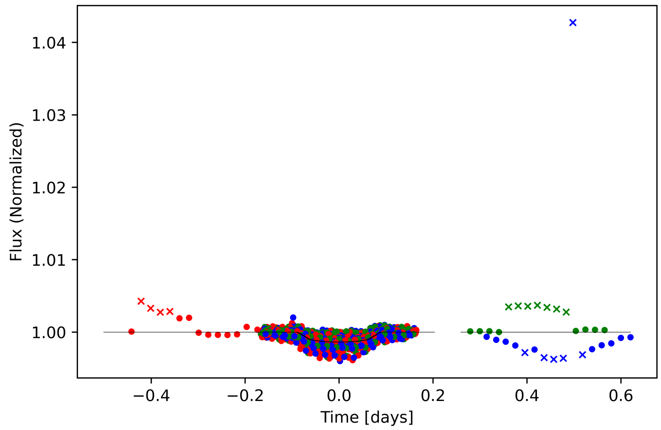

Figure 9. Deterending Lightcurve for the long-cadence Koi 46.01. The x-axis represents the lasting of each transit in the unit of days, the y-axis represents the normalized flux from the star. Every dot represents a data point from the Kepler telescopes and different colors marked the data points from different transit. The dark lines are the best fit model of each transits.The outliers that are 5 σ away are marked as cross (x). We observe there is a data point within the upper right corner obtain 1.04 normalized flux

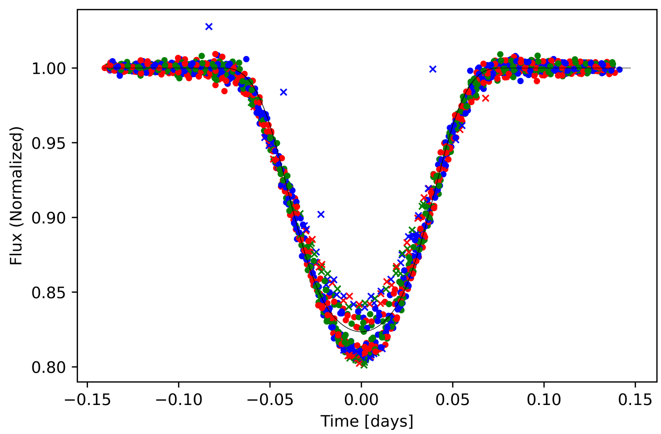

Figure 10. Deterending Lightcurve for the long-cadence Koi 3542.01. The x-axis represents the lasting of each transit in the unit of days, the y-axis represents the normalized flux from the star. Every dot represents a data point from the Kepler telescopes and different colors marked the data points from different transit. The dark lines are the best fit model of each transits.The outliers that are 5 σ away are marked as cross (x). We can observe few transits has been marked as outliers, and removed from calculations

Zhu, W., & Dong, S. 2021, ARA&A, 59, 291, doi: 10.1146/annurev-astro-112420-020055

Zhu, W., Petrovich, C., Wu, Y., Dong, S., & Xie, J. 2018, ApJ, 860, 101, doi: 10.3847/1538-4357/aac6d5

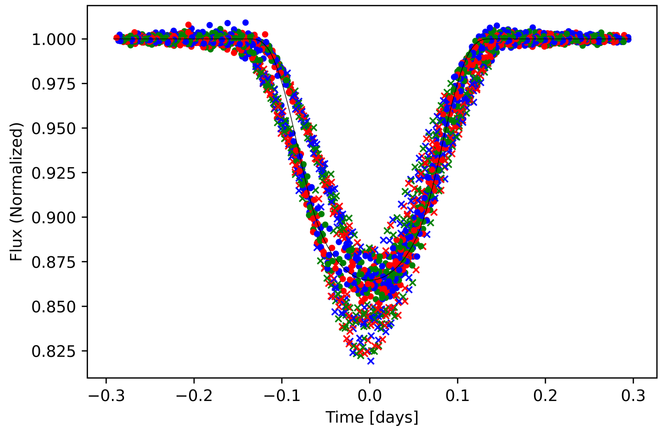

Figure 11. Deterending Lightcurve for the long-cadence Koi 3609.01. The x-axis represents the lasting of each transit in the unit of days, the y-axis represents the normalized flux from the star. Every dot represents a data point from the Kepler telescopes and different colors marked the data points from different transit. The dark lines are the best fit model of each transits.The outliers that are 5 σ away are marked as cross (x). We can observe multiple transits has been marked as outliers, and removed from calculations

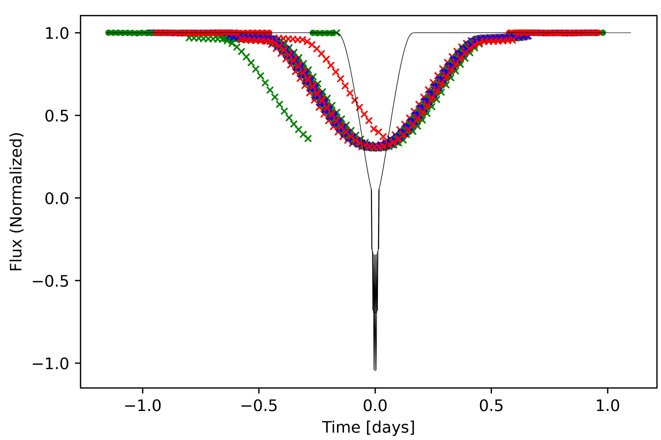

Figure 12. Deterending Light curve for the long-cadence Koi 6933.01 The x-axis represents the lasting of each transit in the unit of days, the y-axis represents the normalized flux from the star. Every dot represents a data point from the Kepler telescopes and different colors marked the data points from different transit. The dark lines are the best fit model of each transits.The outliers that are 5 σ away are marked as cross (x). We observe the changing of flux is more than 0.5 of the normalized value, which is clearly not a transiting planets